JOURNAL OF Applied Polymer SCIENCE

Anion Exchange Membranes Based on Poly(vinyl alcohol) and Quaternized Polyethyleneimine for Direct Methanol Fuel Cells

Pei Yu Xu, Tian Yi Guo, Chun Hui Zhao, Ian Broadwell, Qiu Gen Zhang, Qing Lin Liu
Department of Chemical and Biochemical Engineering, National Engineering Laboratory for Green Chemical Productions of Alcohols, Ethers and Esters, The College of Chemistry and Chemical Engineering, Xiamen University, Xiamen 361005, China
Correspondence to: Q. L. Liu (E-mail: qlliu@xmu.edu.cn)

ABSTRACT: The semi-interpenetrating polymer network technique was applied in the preparation of anion exchange membranes for direct methanol fuel cells (DMFCs). Poly(vinyl alcohol) was chosen as the polymer matrix and quaternized polyethyleneimine was used as the cationic polyelectrolyte. To modify the polymer membranes for achieving desirable properties, 1,2-bis(triethoxysilyl) ethane was used as a precursor to fabricate a set of organic–inorganic hybrid membranes. The hybrid membranes were characterized using X-ray diffraction, scanning electron microscopy, and thermogravimetric analysis. The ionic conductivity, methanol permeability and stability under oxidative and alkaline conditions were measured to evaluate the applicability in DMFCs. © 2012 Wiley Periodicals, Inc. J. Appl. Polym. Sci. 128: 3853–3860, 2013

KEYWORDS: membranes; blends; composites

Received 6 July 2012; accepted 19 September 2012; published online 12 October 2012
DOI: 10.1002/app.38592

INTRODUCTION

Direct methanol fuel cells (DMFCs) have attracted considerable attention as a power source due to various advantages including high energy density, compact design, and low emission. One of the key components in DMFCs is the solid polymer electrolyte. Two types of solid polymer electrolyte have been studied in DMFCs: proton exchange membranes (PEMs) and anion exchange membranes (AEMs). Most DMFCs use proton exchange membranes, such as Nafion® from DuPont. They show excellent chemical, mechanical, and thermal stability and high ionic conductivity. Unfortunately, several technical drawbacks such as slow oxidation kinetics of methanol and high methanol crossover from the anode to the cathode impede their application in DMFCs.[1,2]

To overcome the problems of PEMs, there has been a growing interest in developing AEMs for fuel cell applications.[3–6] AEM fuel cells have several advantages over PEM counterparts: (1) the inherently faster kinetics of oxygen reduction reactions in an alkaline fuel cell allows low cost non-noble metal electrocatalysts such as Ag and Ni to replace traditional Pt. (2) The direction of the ion transport in the AEMs is opposite to that of the methanol thus reducing methanol permeability. (3) The simplified water management and less-corrosive nature of an alkaline environment ensure a potential greater longevity.[7–9]

A variety of approaches for AEM preparation have been attempted. Those include (1) ion-solvating,[10–12] Hou et al. developed a class of AEM by doping KOH in polybenzimidazole (PBI) membrane, the ionic conductivity of the membrane reached up to 0.0184 S cm^{-1}.[10] However, low material stability was observed due to KOH release from the matrix. (2) Introducing cationic moieties by chemical grafting,[3,13–16] for example, Wang et al. prepared AEMs by tethering a chloromethyl pendant group onto poly(ether-imide), the ionic conductivity was up to 0.0351 S cm^{-1} but the use of carcinogenic substance chloromethyl methyl ether limited their application.[16] (3) Radiation-induced grafting,[17–19] Varcoe et al. prepared AEMs by radiation-induced graft polymerization of chloromethyl styrene onto fluorinated ethylene propylene membranes with conductivity up to 0.023 S cm^{-1} at 50°C,[18] however, the high cost of the membranes makes them hard to be cost effective for use in DMFCs. AEMs also have the inherent defect of low ionic conductivity (mobility of OH^- is only 1/2–1/3 of that of H^{+}[20]). Clearly, there is an urgent need to develop novel anion exchange membranes with similar performances levels to match traditional proton exchange membranes, such as Nafion in DMFCs applications.

Semi-interpenetrating polymer network (s-IPN) is currently attracting great attention due to its good mechanical strength and easy preparation.[21–24] When s-IPN is used as an ion exchange membrane, the polyelectrolyte immobilized in a crosslinked

Additional Supporting Information may be found in the online version of this article.

Applied Polymer SCIENCE

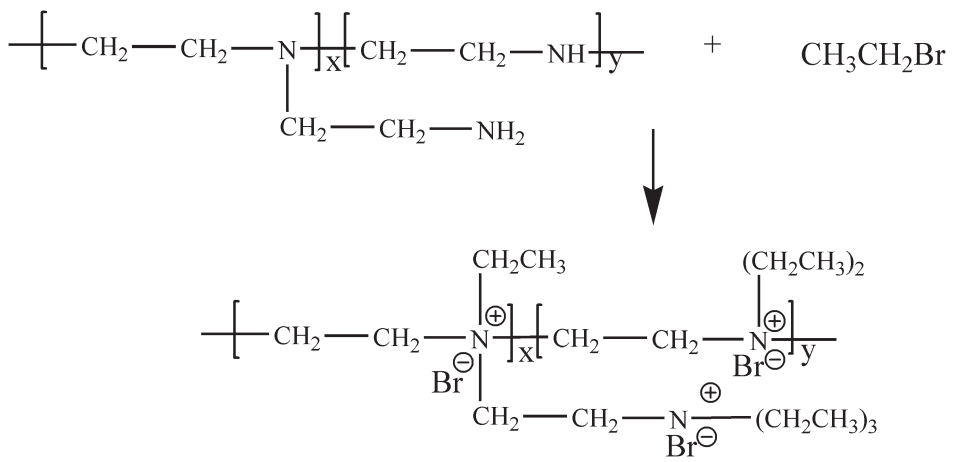

Scheme 1. Schematic representation for preparing QPEI (The symbol of *x* and *y* is polymerization degree).

polymer network matrix is responsible for the ion exchange characteristic.[25] In this article, we prepared anion exchange membranes in which poly(vinyl alcohol) (PVA) was chosen as a polymer matrix due to its good film-forming abilities and good methanol diffusion resistance. Bromoethane-treated PEI was used as a polyelectrolyte. Because PEI has a mass of nitrogen atoms of amine groups on its polymer chains, and can provide plenty of anion exchange groups after modification by bromoethane (Scheme 1).[26] The characteristics of the organic–inorganic membranes were evaluated for potential application in alkaline DMFCs.

MATERIAL AND METHODS

Materials

PVA (M_w 89,000–98,000, 99+% hydrolyzed PVA), branched polyethyleneimine (PEI, M_w 25,000 g mol^{-1}) and 1,2-bis(triethoxysilyl)ethane (BTESE) were purchased from Sigma–Aldrich. All other solvents and reagents of analytical grade were purchased from Sinopharm Chemical Reagent, and used without further purification.

Synthesis of PVA-Based Organic–Inorganic Hybrid Material

PVA was dissolved in dimethylsulfoxide (DMSO) and stirred at 90°C for 2 h. To form mobile silica fragments rather than large particles, a certain amount of BTESE precursor was added drop by drop while stirring at 60°C for 3 h. This was added to enhance the mechanical strength and hydrothermal stability of the final polymer. Next the hot solution was filtrated and the pH was adjusted to 5.00 using 1*M* HCl.

Synthesis of Quaternized PEI

Branched PEI was dissolved in DMSO to obtain a 5 wt % solution. Then a certain amount of bromoethane (see below for detail) was added into the solution and stirred at 60°C for 1 h to obtain clear homogeneous quaternized PEI (QPEI) solution.

Membrane Preparation

The QPEI solution was added into the PVA solution, 40 wt % QPEI content was calculated on the basis of solvent-free. Then 2 mL of 10 wt % GA was added as a crosslinking reagent.[27] The membranes were dried at 40°C for 48 h to remove the solvent, peeled off and further dried in a vacuum oven at 100°C for 4 h. The membranes were then soaked into 1*M* KOH solution at 30°C for 24 h and washed with deionized water until the pH was neutral. The obtained hybrid membranes are termed as PB-X-Y, where X is the percentage ratio of bromoethane to branched PEI and Y is that of BTESE to PVA, being set at 0, 1, 2, 3, 4, 6, 8, 10, and 15.[28] The effects of bromoethane and BTESE content are discussed in this work.

Characterizations

Physical and Chemical Structure. The physical structure of the membranes was studied by X-ray powder diffraction (XRD; Panalytical X'pert, Enraf-Nonious, Holland) using Cu Kα radiation in the range 10–80° at a speed of 0.167° s^{-1}. The chemical structure of the membranes was characterized using a Fourier transform infrared spectrometer (Nicolet Avatar 330, Thermo Electron Corporation).

Thermal Properties. The thermal properties of the membranes were measured using a thermo gravimetric analyzer (TGA, TG209F1, NETZSCH, Germany) under an nitrogen atmosphere in a temperature range 30–900°C with a heating rate of 10°C min^{-1}.

Water Content and Ion Exchange Capacity. To determine the properties of different forms of water in the polymer, the content of free water and bound water in the membranes was measured.[29,30] The membrane samples in hydroxide form were first placed in deionized water at 30°C for 24 h to ensure sufficient water molecules to be attached onto the polar and ionic groups. The mass of hydrated membranes (m_{wet}) was measured as soon as the surface-attached water was removed with filter paper. Then the hydrated membranes were dried at 30°C for 48 h to remove the free water and weighed to obtain the mass (m_{bound}). Afterward the membranes were further heated in vacuum oven at 80°C until a constant mass (m_{dry}). The water uptake is calculated by

$$\text{Bound water uptake} = \frac{m_{bound} - m_{dry}}{m_{dry}}$$

$$\text{Free water uptake} = \frac{m_{wet} - m_{bound}}{m_{dry}}$$

$$\text{Total water uptake} = \text{Free water uptake} + \text{Bound water uptake}$$

Ion exchange capacity (IEC) of the membranes was measured by the classical back titration method. Membranes in hydroxide

form were stirred in 100 mL of 0.1*M* HCl aqueous solution at 30°C for 48 h to ensure a complete exchange. The solutions were then back titrated with 0.1*M* NaOH aqueous solution using phenolphthalein as an indicator. Blank sample of 0.1*M* HCl aqueous solution was also back titrated with the NaOH aqueous solution for the correction of IEC. The IEC value (meq g^{-1}) is calculated by,

$$\mathrm{IEC} = \frac{M_{\mathrm{NaOH}} \times \left(V_{\mathrm{O,NaOH}} - V_{\mathrm{e,NaOH}}\right)}{m_{\mathrm{dry}}}$$

where M_{NaOH} is the concentration of the NaOH aqueous solution (mmol mL^{-1}), $V_{\mathrm{o,NaOH}}$ and $V_{\mathrm{e,NaOH}}$ are the volumes of the NaOH aqueous solution required to titrate the sample and the blank, respectively (mL), m_{dry} is the mass of dry membranes in hydroxide form (g).

Ionic Conductivity Measurements. The ionic conductivities of the membranes in hydroxide form were measured in the temperature range 30–80°C by two-probe AC impedance spectroscopy using Parstat 263 electrochemical equipment (Princeton Advanced Technology) over the frequency range 0.1 Hz–1 MHz. The membranes were tightened by screws to ensure good contact with two stainless steel electrodes. The membranes and the electrodes were set in a glass cell. The cell was placed in a temperature-controlled chamber containing a deionized water reservoir to maintain the relative humidity of 100% throughout each experiment. The ionic conductivity σ (S cm^{-1}) is calculated by,

$$\sigma = \frac{l}{R_m \times A}$$

where l is the distance between the two stainless steel electrodes (cm), R_m is the membrane resistance from the AC impedance data (Ω), and A is the cross-sectional area of the membranes (cm^2).

Methanol Permeability. The methanol permeability was measured using a home-made diffusion cell. In the test, the cell was placed in a thermostatic water bath. The cell comprises two identical compartments separated by a membrane sample tightened by screw clamps. Compartment A was filled with 2*M* aqueous methanol solution[31] and compartment B was filled with deionized water. Both compartments were stirred to ensure uniform concentrations of methanol during the test. Before testing, the membrane samples in hydroxide form were soaked in deionized water for 24 h. The methanol concentration in compartment B was measured over time with gas chromatography (GC-950, Shanghai Haixin Chromatographic Instruments). And the methanol permeability P (cm^2 cm^{-1}) can be estimated as follows,

$$C_B(t) = \frac{A_m}{l_m}\frac{P}{V_B} C_A(t - t_o)$$

where C_A and $C_B(t)$ are the concentration of methanol in compartment A and B (mol L^{-1}), respectively, A_m is the effective area of the membrane (cm^2), l_m is the thickness of hydrated membrane sample (cm), and V_B is the volume of the solution in compartment B.

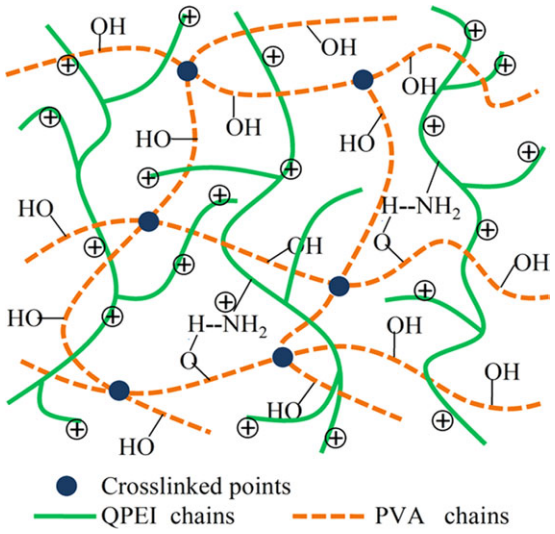

Figure 1. Structure of the s-IPN polymer of PVA and QPEI. [Color figure can be viewed in the online issue, which is available at wileyonlinelibrary.com.]

Mechanical Property and Stability under Oxidative and Alkaline Conditions. The oxidative stability was studied by observing the variation in the weight and conductivity of the membranes in Fenton's reagent.[32] Membrane samples were first immersed in deionized water at 60°C to achieve a swelling equilibrium then placed into Fenton's reagent (4 ppm $FeSO_4$ in 3% H_2O_2) at 60°C. The samples were taken out of the solution at regular intervals and quickly weighed after removing the surface liquid with filter paper. The Fenton's reagent was refreshed every 10 h. The mechanical property measurement can be found in Supporting Information. Stability under alkaline conditions was studied by immersing the membrane samples into NaOH aqueous solutions at 60°C for 24 h. The samples were taken out to measure their conductivity.

RESULTS AND DISCUSSION

Membrane Preparation

The concept of the s-IPN is schematically illustrated in Figure 1. The branched QPEI was interpenetrated in the crosslinked PVA chains to form the s-IPN structure. The unreacted ternary amine groups could form hydrogen bonding with PVA to provide extra anion exchange groups to the membranes. The bromoethane content plays an important role in fabricating the membranes. It has a dominant influence on the mechanical strength and ionic conductivity of the membranes. The ionic conductivity as a function of ion exchange capacity and water content is measured to get desirable PVA/QPEI blending membranes without sacrificing mechanical strength.

As an important character in ion exchange membranes, IEC was strongly affected by C_2H_5Br content (Table I). Membrane (PB-0-0) prepared without bromination exhibited a very low IEC (0.73 meq g^{-1}). IEC increased significantly with increasing C_2H_5Br content. However, when the bromination reaction is approaching complete IEC tends to a constant with increasing C_2H_5Br content further progressively. The hydrophilicity of the membranes was reduced by introducing alkyl groups via

Applied Polymer SCIENCE

Table I. Water Uptake and *IEC* of the s-IPN Membranes

Membrane	C_2H_5Br (wt %)	BTESE (wt %)	Water uptake (%)	IEC (meq g^{-1})
PB-0-0	0	0	117.8	0.73
PB-10-0	10	0	115.3	1.30
PB-20-0	20	0	98.2	1.59
PB-30-0	30	0	103.6	2.03
PB-35-0	35	0	115.8	2.25
PB-40-0	40	0	120.9	2.21
PB-35-6	35	6	82.3	2.32
PB-35-15	35	15	99.5	2.28

bromination reaction, resulting in a slight decrease in water content. It was then increased with quaternization proceeding further. Thus, the optimal value of 35 wt % QPEI was used considering that a phase separation occurred and mechanical strength of the membrane decreased significantly with increasing QPEI content further. With considering both water uptake and IEC values (Table I), three samples of PB-35-0, PB-35-6 and PB-35-15 with higher performance were used to characterize the transport properties, thermal stability, ionic conductivity, etc.

Chemical Structure

FTIR spectroscopy is applied to identify the functional groups in the hybrid membranes to provide the evidence of the reaction mentioned above. Figure 2 shows FTIR spectra of the membranes with the addition of different percentages of BTESE. The silica network was formed by the reaction between hydroxide group of PVA and that of BTESE after acid-catalyzed hydrolysis. It was verified by IR that the contributions associated with stretching of Si—O—Si and Si—O—C groups are the peaks of 1095 and 1021 cm^{-1},[28,33,34] respectively. With increasing BTESE contents, the peaks increased resulting from BTESE self-condensation. Crosslinking reaction occurred between hydroxide group of PVA and aldehyde group of GA used as a chemical crosslinking agent. With the same amount of crosslinking agent, the reaction was proceeded accompanying with a decrease in the intensity of the absorption bands at 2846 cm^{-1} (characteristic of —CHO, aldehyde group) and 3372 cm^{-1} (characteristic of —OH group and the possibly bound water).[35] This indicates that the Si—C—C—Si segments can stretch the s-IPN structure so that the reaction can take place easily due to less steric hindrance.[28] However, the peaks increased with further increasing BTESE content. This is thought to be caused by the formation of large silica particles during hydrolysis and self-condensation of BTESE. As a consequence, when a sufficient amount of BTESE was incorporated into the PVA matrix the large particles twined around the PVA chains that intensified the space steric effect.

Thermal Stability

The thermal properties of the membranes are illustrated by their TGA studies (Figure 3). The weight loss curves of PB-35-0, PB-35-6, and PB-35-15 could be divided into four stages at around 30–200, 200–400, 400–470, and 470–600°C. In the initial stage, the loss was associated with the evaporation of bound

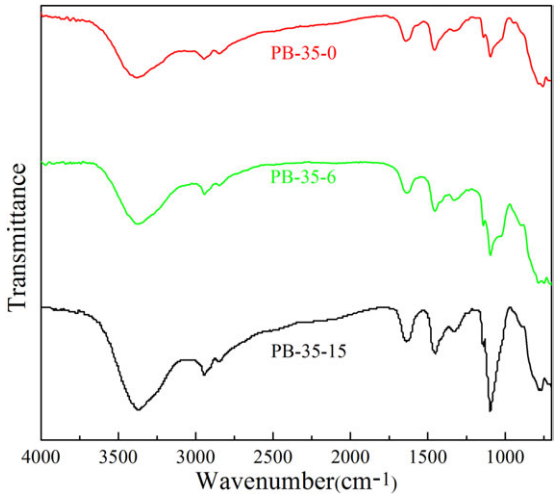

Figure 2. FT-IR spectra of membranes (a) PB-35-0, (b) PB-35-6, and (c) PB-35-15. [Color figure can be viewed in the online issue, which is available at wileyonlinelibrary.com.]

water and the water absorbed onto the s-IPN membranes from the air. It should be noted that the weight of water in PB-35-6 decreased slower than that in the others. The phenomenon stemmed from the fact that the water molecules have been bounded tightly to PB-35-6 via hydrogen bonding due to the free space formed from the condensation reaction between PVA and BTESE. The second stage (200–400°C) was attributed to the decomposition of bromomethyl groups in the PEI chains. In the third stage, the PVA chains split into small segments by the thermal treatment from 400 to 470°C. The last stage associated with the pyrolysis of BTESE would lead to a slight loss in weight ranging from 470 to 600°C. The fact that more residues were left after heat treatment is evidence for large inorganic particles forming within the s-IPN structure with increasing BTESE content. Figure 3 shows that the weight loss of PB-35-0 is greater than that of the others in which an inorganic phase was

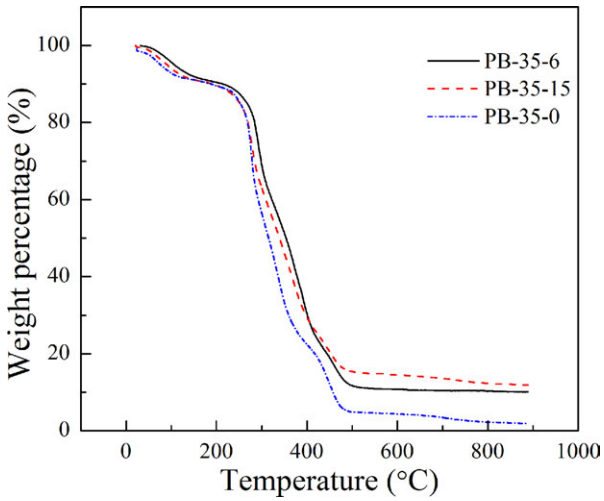

Figure 3. TGA curves of membranes (a) PB-35-0, (b) PB-35-6, and (c) PB-35-15. [Color figure can be viewed in the online issue, which is available at wileyonlinelibrary.com.]

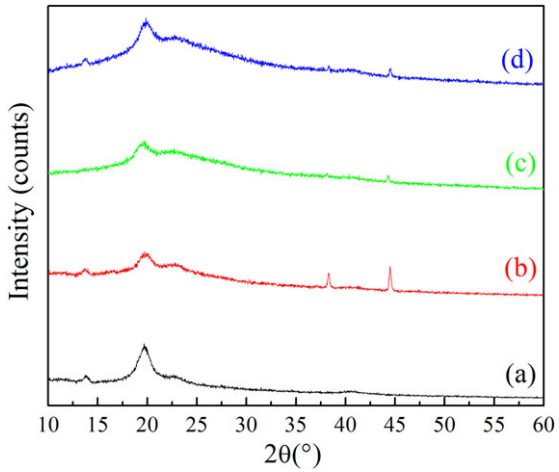

Figure 4. XRD patterns of membranes (a) PVA, (b) PB-35-0, (c) PB-35-6, and (d) PB-35-15. [Color figure can be viewed in the online issue, which is available at wileyonlinelibrary.com.]

introduced. This suggests that the incorporation of silica moiety into s-IPN membranes can successfully improve their thermal stability. This is because incorporation of an inorganic component into a polymer matrix can normally improve the thermal stability of the resulting hybrid.

Structure Characteristic of the s-IPN Membranes

Figure 4 shows the crystalline phase of the membranes characterized by XRD. A diffraction peak of PVA appeared at $2\theta = 20°$. A decrease in the peak intensities from PVA to PB-35-0 suggests that PVA/QPEI s-IPN structure could prevent the formation of crystalline region in the PVA matrix. The peak appeared at $2\theta = 44°$, when QPEI was interpenetrated into the PVA chains [Figure 4(b)], indicates a new crystalline region being formed. The peak in Figure 4(c) is broader than that in Figure 4(b). This suggests the introduction of silica moiety leading to a decrease in the crystallinity. The result could be attributed to a decrease in the hydroxyl groups in the membrane resulting from the condensation between silica and PVA. The ion transport process will be much easier when the crystallinity decreased and thus higher ionic conductivity could be achieved. Figure 4(d) shows a sharper peak due to the large inorganic particles aggregating instead of dispersing between the PVA chains. The structure is also confirmed by the morphology characterization using scanning electron microscope (see Supporting Information Figure S1).

Water Content

Two forms of water (free water and bound water) dependent of the interaction between water and polymer generally exist. Attached to the ionic and polar groups on the polymer chains, bound water plays an important role in transporting the hydroxide ions in the membrane. The water, having the same phase transition temperature as the bulk water, is designated as free water.[29] Clusters of the free water are the bound water supply station. Thus, a great amount of attainable water in the membrane is desirable. Figure 5(a) shows the free and bound water uptake as a function of BTESE content. The heating of the membranes in the hydroxide formed at 80°C to constant weight can lead to conservative values of free and bound water uptake due to decomposition of the quaternary ammonium groups, accompanied by the release of low molecular weight degradation products. Probably, this explains high values of bound water uptake (40–80 wt %).

The BTESE-induced inorganic phase in the membrane reduces the water uptake of the membrane but has slight effect on the IEC. This is because ion exchange groups do not vary upon introduction of silica in the membranes and quaternary ammonium groups are influenced slightly by hybrid structure. With increasing BTESE content, the tethered Si—C—C—Si segments cause the s-IPN structure more compact.[28] The compact structure with small silica particles may reduce the hydrophilicity of membranes leading to a decrease in total water uptake. As a result, total water uptake decreased dramatically from 115.8 to 82.3%. However, it should be noted that bound water arises from —OH groups in PVA chains and Si—OH groups induced by the self-condensation. The ratio of bound water to total water uptake incresead leading to an increase in ionic conductivity [Figure 5(b)]. This is because efficient bound water attached to the ionic and polar groups is favorable for the hydroxide ions to transport through the membranes. With increasing BTESE content further, the ratio of bound water to total water uptake dramatically decreased since the rate of self-condensation was faster than that of condensation between hydroxide groups in PVA chains and BTESE. The reason for a decrease in bound water is thought to be due to microphase separation that occur between silica-rich domains and the organic polymer matrix. Thus the ionic conductivity was too low to meet the requirement of DMFCs.

Ionic Conductivity

From Figure 6 we see that conductivity of the hybrid membranes scales linearly as a function of temperature for 30–80°C in deionized water. The ionic conductivity was greater than 2.2 $\times$ 10^{-2} S cm^{-1} for PB-35-6 and PB-35-0. PB-35-6 showed

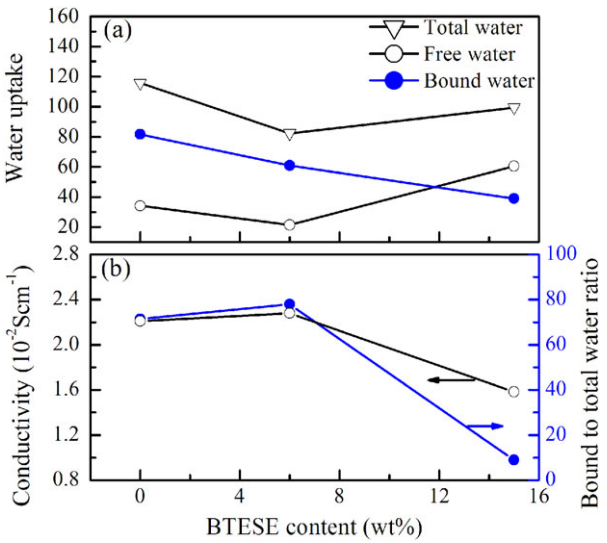

Figure 5. Effect of BTESE content on the free and bound water uptake, and ionic conductivity. [Color figure can be viewed in the online issue, which is available at wileyonlinelibrary.com.]

Applied Polymer SCIENCE

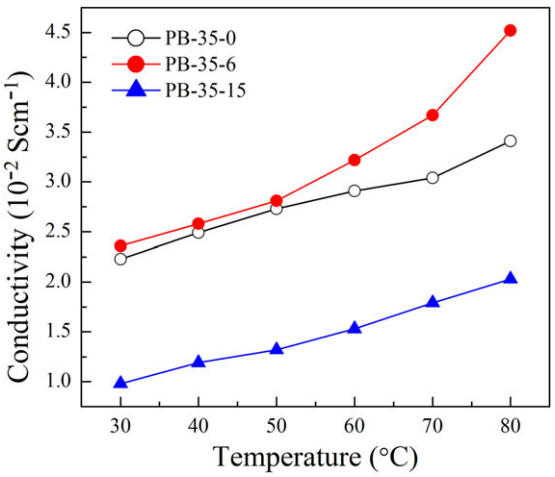

Figure 6. Ionic conductivity of the three s-IPN membranes vs. temperature. [Color figure can be viewed in the online issue, which is available at wileyonlinelibrary.com.]

a conductivity of 2.36×10^{-2} S cm^{-1} at 30°C and could reach the maximum OH^- conductivity of 4.52×10^{-2} S cm^{-1} at 80°C. This is desirable in contrast with the reported anion exchange membranes and can meet the requirement of DMFCs. The conductivity of PB-35-6 and PB-35-0 was much higher than that of PB-35-15, indicating self-condensation induced large particles act as obstacles to ion transport within the membrane. Although both PB-35-0 and PB-35-6 have a similar IEC, the ionic conductivity of PB-35-6 is larger than that of PB-35-0. This may be due to the increase of the amorphous region (Figure 4) which could facilitate the ion transport.

Methanol Permeability

Figure 7 shows the methanol permeability of the s-IPN Membranes in 2*M* methanol solution vs. temperature. Methanol permeability increased with increasing temperature. This results from an increase in the mobility of both methanol and polymer chains with increasing temperature. The methanol permeability of PB-35-0 was considerably higher than that of PB-35-6 in the temperature range 30–70°C. This suggests that blockage of the methanol molecules from the Si—C—C—Si segments results in a decrease in the mobility of methanol molecules when the silica network stretched the s-IPN structures to a certain degree.[28] The occupied volume of the tethered Si—C—C—Si segment (83.59 Å^3/unit segment) is larger than that of the original Si—O—Si segment (67.36 Å^3/unit segment).[36] In this situation, incorporation of BTESE would reduce the free volume of the as-prepared AEMs leading to a lower methanol permeability. PB-35-15 exhibited higher methanol permeability than PB-35-6. The self-condensation induced large inorganic clusters will facilitate micro phase separation to form a large amount of free space acting as the methanol transporting channels. Nafion® 115 exhibits methanol permeability of 2.23×10^{-6} cm^2 s^{-1} at 30°C.[37] The PB-35-6 presents a value of 0.78×10^{-6} cm^2 s^{-1} at 30°C, about 1/3 of the Nafion membrane. This makes it have a potential application in DMFCs.

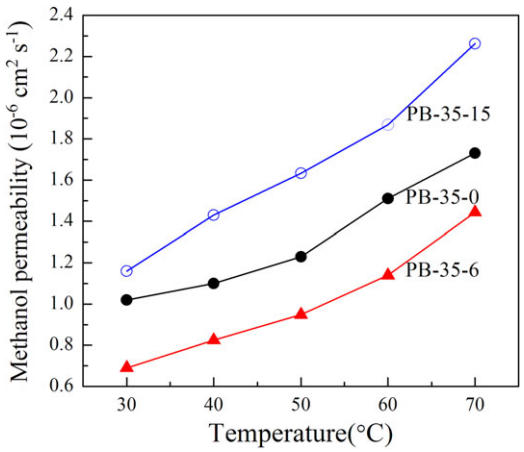

Figure 7. Methanol permeability of the three s-IPN membranes vs. temperature. [Color figure can be viewed in the online issue, which is available at wileyonlinelibrary.com.]

Mechanical Property and Stability under Oxidative and Alkaline Conditions

High oxidative stability of polymer electrolyte membranes is required for DMFCs application. Fenton's reagent was chosen to simulate the practical operation environment of fuel cells. Figure 8 shows the evolution of weight and ionic conductivity of PB-35-6. The weight of the membranes gradually decreased with time. The membrane had a 21.7% weight loss after 120 h. This weight loss is attributed to the degradation of quaternary ammonium groups. The ionic conductivity of the PB-35-6 membrane before and after the oxidative testing is 3.22×10^{-2} and 2.68×10^{-2} S cm^{-1}, respectively. The oxidative stability is acceptable in contrast with some other anion exchange membranes.[38] It is known that the main way of destruction of AEMs is degradation of quaternary ammonium groups by OH^- nucleophilic attack.[8] In this case different rearrangements and degradation mechanisms take place. One of them is the cleavage of the quaternary ammonium by OH^- followed by elimination (called as Hofmann degradation or E2 elimination). Therefore, investigation of

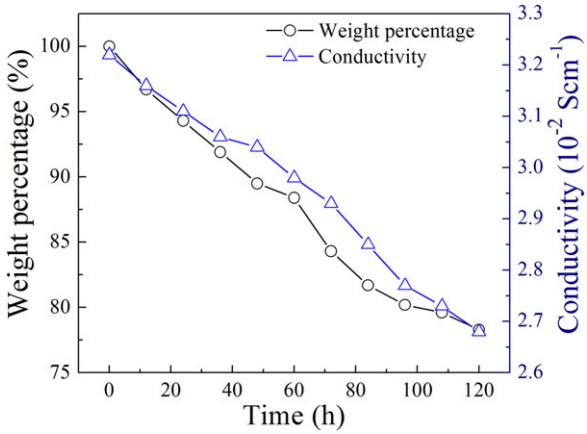

Figure 8. Chemical stability of PB-35-6 membrane in a Fenton's reagent at 60°C. [Color figure can be viewed in the online issue, which is available at wileyonlinelibrary.com.]

membranes stability under alkaline conditions is of higher priority. The ionic conductivity of the PB-35-6 membrane immersed into 2–10 mol L^{-1} NaOH aqueous solution is 2.58–2.22 $\times$ 10^{-2} S cm^{-1}. The membrane stability is slightly sensitive to NaOH concentration (see Supporting Information Figure S2). Supporting Information Figure S2 shows a slight variation in conductivity and weight percentage of the PB-35-6 membrane immersed in different NaOH concentrations. This suggests that the membrane stability in alkaline media is acceptable. Tensile stress and elongation at break illustrate mechanical properties of the membranes (see Supporting Information Table S1).

CONCLUSIONS

Anion-exchange membranes using PVA as matrix and QPEI as polyelectrolyte were prepared via s-IPN technology. To improve the membrane performance, BTESE was added as a precursor into the s-IPN polymer. Characterizations show that the membranes have a water uptake of 82.3–115.8%, and IEC of 0.73–2.32 meq g^{-1}. TGA analysis indicates that the membranes have thermal degradation above 210°C. The ionic conductivity can reach 4.52 $\times$ 10^{-2} S cm^{-1} at 80°C and methanol permeability of PB-35-6 is in the range 0.78–1.45 $\times$ 10^{-6} cm^2 s^{-1}. This permeability is lower than that of a Nafion® membrane. In summary anion exchange membranes using PVA as matrix and QPEI modification are a potential candidate for future use in alkaline DMFCs. For the time being, though, further work is needed before many of the excellent properties of Nafion will be equaled or superseded.

NOMENCLATURE

A	cross-sectional area of the membrane (cm^2)
A_m	the effective area of the membrane (cm^2)
b	slope of the regression line of $\ln(\sigma)$ vs. $1000/T$ plots
C_A	concentration of methanol in compartment A (mol L^{-1})
C_B	concentration of methanol in compartment B (mol L^{-1})
E_a	ion transport activation energy (kJ mol^{-1})
IEC	ion exchange capacity (meq g^{-1})
l	distance (cm) between two the stainless steel electrodes
l_m	membrane thickness (cm)
$M_{o,HCl}$	milliequivalents (meq) of HCl acquired before equilibrium
$M_{e,HCl}$	milliequivalents (meq) of HCl acquired after equilibrium
P	methanol permeability (cm^2 s^{-1})
R	universal gas constant (8.314 J K^{-1} mol^{-1})
R_m	membrane resistance from the AC impedance data (Ω)
t	time for ending permeability testing (h)
t_0	time for starting permeability testing (h)
V_A	volume of the solution in compartment A (cm^3)
W_{wet}	weight of wet membrane (g)
W_{dry}	weight of dry membrane (g)

ACKNOWLEDGMENTS

Financial support from National Nature Science Foundation of China Grant Nos. 20976145 and 21076170, Nature Science Foundation of Fujian Province of China Grant Nos.2009J01040 and 2010I0013, and the research fund for the Doctoral Program of Higher Education (No. 20090121110031) in preparation of this article is gratefully acknowledged. We are greatly thankful for the referees' helpful comments.

REFERENCES

1. Ketelaar, J. A. A.; Blomen, L. J. M. J.; Mugerwa, M. N. Fuel Cell Systems; Plenum Press: New York, **1993**.
2. Vielstich, W.; Lamm, A.; Hubert, A. G. Handbook of Fuel Cells: Fundamentals, Technology, Applications; Wiley: Chichester; **2003**, p 351.
3. Wang, G. G.; Wang, Y.; Chu, D.; Chen, R. *J. Membr. Sci.* **2009**, *332*, 63.
4. Fujiwara, N.; Siroma, Z.; Yamazaki, S. I.; Ioroi, T.; Senoh, H.; Yasuda, K. *J. Power Sources* **2008**, *185*, 621.
5. Yu, E. H.; Scott, K. *J. Power Sources* **2004**, *137*, 248.
6. Guo, T. Y.; Zeng, Q. H.; Zhao, Q. H.; Liu, Q. L.; Zhu, A. M.; Broadwell, I. *J. Membr. Sci.* **2001**, *371*, 268.
7. Prabhuram, J.; Manoharan, R. *J. Power Sources* **1998**, *74*, 54.
8. Varcoe, J. R.; Slade, R. C. T. *Fuel Cell* **2005**, *5*, 187.
9. Tripkovic, A. V.; Popovic, K. D.; Grgur, B. N.; Blizanac, B.; Ross, P. N.; Markovic, N. M. *Electrochim. Acta* **2002**, *47*, 3707.
10. Hou, H.; Sun, G.; He, R.; Wu, Z.; Sun, B. *J. Power Sources* **2008**, *182*, 195.
11. Modestov, A. D.; Tarasevich, M. R.; Leykin, A.; Filimonov, V. *J. Power Sources* **2009**, *188*, 502.
12. Wan, Y.; Creber, K. A. M.; Peppley, B.; Bui, V. T. *J. Membr. Sci.* **2006**, *284*, 331.
13. Li, L.; Wang, Y. *J. Membr. Sci.* **2005**, *262*, 1.
14. Xing, D. B.; Zhang, S. H.; Yin, C. X.; Yan, C.; Jian, X. G. *Mater. Sci. Eng. B* **2009**, *157*, 1.
15. Tripathi, P.; Kumar, M.; Qumar, M.; Shahi, V. K. *J. Membr. Sci.* **2010**, *360*, 90.
16. Wang, G.; Wang, Y.; Chu, D.; Xie, D.; Chen, R. *J. Membr. Sci.* **2009**, *326*, 4.
17. Varcoe, J. R.; Slade, R. C. T. *Electrochem. Commun.* **2006**, *8*, 839.
18. Slade, R. C. T.; Varcoe, J. R. *Solid State Ionics* **2005**, *176*, 585.
19. Matsuoka, K.; Iriyama, S.; Abe, Y.; Matsuoka, T.; Kikuchi, M. *Thin Solid Films* **2008**, *516*, 3309.
20. Varcoe, J. R. *J. Phys. Chem. B* **2007**, *9*, 1479.
21. Choi, Y. J.; Kang, M. S.; Moon, S. H. *J. Appl. Polym. Sci.* **2002**, *88*, 1488.
22. Prakash, G.; Smart, M.; Wang, Q.; Atti, A.; Pleynet, V. *J. Fluorine Chem.* **2004**, *125*, 1217.

23. Cho, K. Y.; Jung, H. Y.; Shin, S. S.; Choi, N. S. *Electrochim. Acta* **2004**, *50*, 589.
24. Walker, C. W. *J. Electrochem. Soc.* **2004**, *42*, 1797.
25. Lebrun, L.; Follain, N.; Metayer, M. *Electrochim. Acta* **2004**, *50*, 985.
26. Chachulski, B.; Gebicki, J.; Jasinski, G.; Jasinski, P.; Nowakowski, A. *Meas. Sci. Technol.* **2006**, *17*, 12.
27. Yeom, C. K.; Lee, K. H. *J. Membr. Sci.* **1996**, *109*, 257.
28. Zhang, Q. G.; Liu, Q. L.; Zhu, A. M.; Xiong, Y.; Zhang, X. H. *J. Phys. Chem. B* **2008**, *112*, 16559.
29. Kim, D. S.; Park, H. B.; Rhim, J. W.; Lee, Y. M. *J. Membr. Sci.* **2004**, *240*, 37.
30. Zawodzinski, T. A.; Springer, T. E.; Davey, J.; Jestel, R.; Lopez, C.; Valerio, J.; Gottesfeld, S. *J. Electrochem. Soc.* **1993**, 140, **1982**.
31. Zhu, X.; Zhang, H.; Liang, Y.; Zhang, Y.; Luo, Q.; Bi, C.; Yi, B. *J. Mater. Chem.* **2007**, *17*, 386.
32. Xiong, Y.; Fang, J.; Zeng, Q. H.; Liu, Q. L. *J. Membr. Sci.* **2008**, *311*, 319.
33. Mansur, H. S.; Orefice, R. L.; Mansur, A. A. P. *Polymer* **2004**, *45*, 7193.
34. Liu, Y. L.; Su, Y. H.; Lai, J. Y. *Polymer* **2004**, *45*, 6831.
35. Speight, J. G. Lange's Handbook of Chemistry; McGraw-Hill: New York, **2005**; p 1244.
36. Chang, K. S.; Yoshioka, T.; Kanezashi, M.; Tsuru, T. *J. Membr. Sci.* **2011**, *381*, 90.
37. Zeng, Q. H.; Liu, Q. L.; Broadwell, I. *J. Membr. Sci.* **2010**, *349*, 237.
38. Wu, Y. H.; Wu, C. M.; Xu, T. W.; Yu, F.; Fu, Y. *J. Membr. Sci.* **2008**, *321*, 299.